phys. stat. sol. (b) **143**, 131 (1987)

Subject classification: 68.30 and 78.65; 71.36; 71.45; S1.3

Sektion Physik der Friedrich-Schiller-Universität Jena[1])

An Improved Virtual Mode Theory of ATR Experiments on Surface Polaritons

Application to Long-Range Surface Plasmon-Polaritons in Asymmetric Layer Structures

By

L. WENDLER and R. HAUPT

The damping properties of surface polaritons, especially long-range surface plasmon-polaritons (LRSP) in asymmetric layer structures are analyzed taking into account the presence of a coupling prism. Both, the response treatment to calculate attenuated-total-reflection (ATR) spectra and the virtual mode treatment are used. Two different types of virtual modes are analyzed. One of them describes the propagation properties of the surface polariton in the presence of both intrinsic and radiative damping. The other type describes a surface polariton with a driving field and hence this mode allows to find out the optimum conditions for the ATR experiment. These two modes are investigated in detail and the results of the numerical calculation are presented in graphical form. The results for the ATR configuration show that in asymmetric embedded silver layers the propagation length exceeds the value for the symmetric embedded one significantly.

Es werden die Dämpfungseigenschaften von Oberflächen-Polaritonen, speziell Langstrecken-Oberflächen-Plasmon-Polaritonen in asymmetrischen Schichtstrukturen unter Einbeziehung der Existenz eines Koppelprismas analysiert. Es werden sowohl die Response-Theorie zur Berechnung der abgeschwächten Totalreflektionsspektren als auch das Konzept der virtuellen Moden verwendet. Zwei verschiedene Typen von virtuellen Moden werden analysiert. Eine von beiden beschreibt die Ausbreitungseigenschaften eines Oberflächen-Polaritons beim Vorhandensein sowohl von intrinsischer als auch Strahlungsdämpfung. Der andere Typ beschreibt ein Oberflächen-Polariton mit einem oszillierenden Feld, womit es diese Mode ermöglicht, optimale Bedingungen für ein Experiment der abgeschwächten Totalreflektion zu finden. Diese beiden Moden werden detailliert untersucht und die Resultate numerischer Rechnungen graphisch dargestellt. Die Ergebnisse für eine Konfiguration zum Experiment der abgeschwächten Totalreflektion zeigen, daß in asymmetrisch eingebetteten Silberschichten die Ausbreitungslänge den Betrag für die symmetrisch eingebettete Silberschicht deutlich überschreitet.

1. Introduction

The surfaces and interfaces always present in real crystals lead to states in the spectra of collective excitations of the solid (phonons, plasmons, excitons, etc.) which differ from that existing in the bulk material. Theoretical studies of these states of the solid and their detection attained a noticeable growing interest and have stimulated the development of new experimental methods. The nondestructive character of optical methods and their sensitivity make them very attractive for use. The method of attenuated total reflection (ATR) [1] and Raman scattering [2] are proved to be especially profitable. In principle a photon bound to the surface or interface of a solid should be very sensitive to the surface properties in comparison to unbound photons

[1]) Max-Wien-Platz 1, DDR-6900 Jena, GDR.

used in the ordinary spectroscopy. This bound photon state is the surface polariton (SP) which is a coupled state of a dipole-active elementary excitation of the solid and a photon [3 to 7].

The excitation of SP's with the ATR method is a resonance phenomenon. The SP will be only excited if both the frequency and the wave vector of the exciting light wave satisfy the dispersion relation of the SP in the present configuration. If the dispersion relation is modified due to the change of the dielectric properties of the system in ATR experiments the SP does not occur any more for these frequency and wave vector values. This leads to an important variation of the quantities which are measured in such experiments. Therefore SP's are suitable for studies of surface properties or as a diagnostic tool in the infrared spectroscopy.

In real solids SP's have a finite damping reflecting the lifetime of the dipole-active elementary excitations of the solid to which the photons are coupled. For the study of the propagation of the SP's along the interface the two prism method is used [8 to 10]. One prism couples SP's into the system and the other decouples them. Measurements [8 to 11] show that the propagation length of surface plasmon-polaritons on the surface of semi-infinite metals in the infrared frequency range is in general of the order of a few centimeters. In thin dipole-active layers sandwiched between two media the physical situation is changed. In such layers in every branch of dipole-active elementary excitations of the medium two SP modes exist. If the thickness of the layer is sufficiently thin their dispersion curves are split. The high-frequency antisymmetric (—) mode called upper mode (UM) and the low-frequency symmetric (—) mode called lower mode (LM) show a different behaviour. It was predicted for thin metallic layers [12, 13] that if the layer is thin enough, the UM is weakly damped in comparison to the LM. The propagation length of the UM can be much larger than the propagation length of the SP in a semi-infinite dipole-active medium. The UM is then called the long-range surface polariton (LRSP) and the LM the short-range surface polariton (SRSP). This is also true for SP's occurring in other than metallic dipole-active layers.

Up to now theoretical investigations were performed also for surface phonon-polaritons in thin dielectric layers [14], surface plasmon-phonon-polaritons [15], and surface magnetoplasmon-polaritons [16] in thin n-type semiconductor layers. But most of the work was done on the LRSP's of thin silver layers [17 to 19]. The remarkable properties of the LRSP's have stimulated theoretical and experimental interest in these SP's. The excitation of the LRSP with the ATR method was demonstrated [20 to 22]. Application the LRSP's to nonlinear effects has received considerable attention [23, 24].

Recently it was shown [25] that in definite asymmetric embedded thin silver layers LRSP's can achieve a propagation length which exceeds the value for the symmetric case by up to three orders of magnitude. However, most of the theoretical studies were performed on LRSP's in an unperturbed system that means on the free oscillations of the three media system superstrate/dipole-active layer/substrate. But the excitation of the LRSP's with the ATR method means that the unperturbed system is accompanied by a coupling prism which is seperated by a gap from the metallic layer. Therefore there is a difference between the free LRSP in the unperturbed configuration superstrate/dipole-active layer/substrate and the excited LRSP in the configuration couple prism/superstrate/dipole-active layer/substrate.

In the present paper we investigate therefore the properties of LRSP's in thin asymmetric embedded silver layers taking into account the effect of the coupling prism. To do this we use two methods, the response theory and the virtual mode theory. Both methods include the damping mechanisms: intrinsic and radiative damping.

The virtual mode theory developed in this paper is suitable to describe both the propagation properties of LRSP's including radiative damping and their optimum excitation in an ATR experiment.

2. Effects of Damping

The system (inset of Fig. 1) we want to consider is the following. The region $z > d + a$ is filled by the coupling prism with the real dielectric constant ε_1. The gap $d + a > z > a$ between the coupling prism and the metal layer is filled by the superstrate with the real dielectric constant ε_2. The metal layer $a > z > 0$ is characterized by a local, homogeneous, isotropic, and frequency-dependent dielectric function $\varepsilon_3(\omega)$ which is a complex function in the presence of intrinsic damping. The region $0 > z$ is filled by the substrate with the real dielectric constant ε_4. Since the media are isotropic we can specialize on waves propagating in the x-direction with the wave vector component $k_{||}$ without loss of generality.

To describe the wave propagation in the above given system for the unpertubed ($d \to \infty$) and undamped (Im $\varepsilon_3 = 0$) system we make use of the boundary conditions at the interfaces for the fields in the four regions of the chosen configuration. The dispersion relation of the SP's is then derived from the condition that the SP may exist without any external driving field. This means the dispersion relation represents a resonance condition which defines the eigenfrequencies $\omega = \omega(k_{||})$ and hence the SP's have an infinite lifetime. Therefore in the presence of damping processes the dispersion relation looses its meaning in this strict sense. The SP's are no longer true normal modes of the system. This is related to the fact that regarding damping processes the solutions ω and $k_{||}$ of the dispersion relation in general will be complex quantities because the dielectric function becomes complex. This means that scattering processes of the elementary excitations serve to couple excitations of different ω–$k_{||}$ points. The dispersion relation for the system has to be fulfilled for complex $\varepsilon_3(\omega)$ that is for both the real and the imaginary part. Consequently the dispersion relation represents two real equations. Because ω as well as $k_{||}$ may be complex there are four variables which are connected by these two equations. Therefore a third relation is necessary to have three variables depending unambiguously on the free running fourth variable. The reason for this lack of information is that for a lossy system the usual periodic boundary conditions in space and time are no more valid and must be replaced by other boundary conditions. There are two principal ways to state boundary conditions:

(i) In the response treatment where the response of the system to an external driving field in the prism region is investigated, one defines conditions on this excitation process.

(ii) A deeper insight into the nature of the physical process which is interested here is obtained from the virtual mode treatment. In this case the excitation process due to intrinsic and radiative damping of a SP in the ATR configuration is separately considered.

Therefore one defines conditions for the excitation process or the radiative exit channel, respectively. That means the states of the system, i.e. the virtual modes (quasi-stationary), correspond to incoming or outgoing waves in the prism region. It is implicitly assumed that the delay between the excitation of the system and its decay is long enough to regard the decay as independent of the excitation of the system.

3. The ATR Response from Surface Polaritons

This section deals with the response function of an experimental ATR set-up [6, 7, 26 to 28]. The linear reflectivity from multilayers in the ATR regime is well-known.

The reflectivity of the coupling prism/superstrate/metal layer/substrate system which is shown in the inset of Fig. 1, may be written as

$$R = |r_{1234}|^2 = \frac{|\boldsymbol{E}^{\mathrm{r}}|^2}{|\boldsymbol{E}^{\mathrm{i}}|^2} \tag{1}$$

with

$$r_{1234} = \frac{r_{12} + r_{234}\, \mathrm{e}^{i2k_{z2}d}}{1 + r_{12}r_{234}\, \mathrm{e}^{i2k_{z2}d}} \tag{2}$$

and

$$r_{234} = \frac{r_{23} + r_{34}\, \mathrm{e}^{i2k_{z3}a}}{1 + r_{23}r_{34}\, \mathrm{e}^{i2k_{z3}a}} \,. \tag{3}$$

Here r_{ij} is the Fresnel reflection coefficient for the p-polarized light, $\boldsymbol{E}^{\mathrm{i}}$ the electric field of the incident wave and $\boldsymbol{E}^{\mathrm{r}}$ that of the reflected wave. The coefficient r_{ij} has the form

$$r_{ij} = \frac{\varepsilon_j k_{zi} - \varepsilon_i k_{zj}}{\varepsilon_j k_{zi} + \varepsilon_i k_{zj}} \,. \tag{4}$$

k_{zi} is the normal component of the wave vector given by

$$k_{zi} = \frac{\omega}{c} (\varepsilon_i - \varepsilon_1 \sin^2 \theta_1)^{1/2} \,. \tag{5}$$

The subscripts $i, j = 1, 2, 3, 4$ refer to the coupling prism, the superstrate, the metal layer, and the substrate, respectively. θ_1 is the angle of incidence.

In this response treatment both θ_1 and ω are real quantities. The minima of the ATR reflectivity (1) or the peaks of the response function $1 - R$ denote the excitations of the system. The wave vector component $k_{||}$ in the direction of propagation of the surface polariton is related to the angle of incidence at the ATR minimum $\theta_1^{\min}$ according to

$$k_{||} = \frac{\omega}{c} \varepsilon_1^{1/2} \sin \theta_1^{\min} \,. \tag{6}$$

In an ATR experiment two possibilities exist to measure a SP resonance:

(i) Angle scan ATR:
The frequency ω is fixed and the angle of incidence θ_1 is varied.
(ii) Frequency scan ATR:
The angle of incidence θ_1 is fixed and the frequency ω is varied.

Performing a frequency scan ATR experiment the detected dispersion curve is qualitatively very similar to that calculated from the dispersion relation without intrinsic damping. Whereas in the case of an angle scan ATR experiment the detected dispersion curve shows a characteristic backbending [29].

4. The Virtual Mode Theory

In the virtual mode theory [6, 21, 30 to 33] the propagation of the modes is regarded to be independent of their excitation. Then we can derive the corresponding dispersion relation from the ATR response function. A finite nonzero response of the system yields the implicit dispersion relation of the surface excitation when the external

electric field $\boldsymbol{E}^{\mathrm{i}}$ is equal to zero. This corresponds to setting the denominator of (1) equal to zero. The resulting dispersion relation takes explicitly into account the influence of the coupling prism. However, to describe the ATR experiment with this dispersion relation for virtual modes we must add to it suitable boundary conditions for the radiative exit channel (see Section 2). For the ATR experiment these conditions follow from the general principle that the fixed variable must be a real quantity but the varied variable will be a complex one.

For the angle scan ω will be real and θ_1 complex. Corresponding to (6) this results in a complex wave vector component $k_{||}$. That means pure spatial damping occurs in the direction of propagation, which is given by the condition

$$\operatorname{Im} \omega = 0 \,. \tag{7}$$

From the simple relation

$$\boldsymbol{k}^{(1)} \cdot \boldsymbol{k}^{(1)} = \varepsilon_1 \frac{\omega^2}{c^2} = \text{real}\,; \qquad \boldsymbol{k}^{(1)} = (k_{||}, 0, k_{z1})$$

it follows that the imaginary cross term $2i \operatorname{Re} \boldsymbol{k}^{(1)} \cdot \operatorname{Im} \boldsymbol{k}^{(1)}$ vanishes. Thus the angle scan experiment is described by virtual modes with $\operatorname{Re} \boldsymbol{k}^{(1)} \perp \operatorname{Im} \boldsymbol{k}^{(1)}$.

In the case of the frequency scan ω will be complex and θ_1 real. From (6) we derive with the complex $k_{||}$ the boundary condition for the frequency scan to

$$\frac{\operatorname{Re} k_{||} + i \operatorname{Im} k_{||}}{\operatorname{Re} \omega + i \operatorname{Im} \omega} = \frac{\varepsilon_1^{1/2}}{c} \sin \theta_1 = \text{real}\,. \tag{8}$$

The consequence is that the frequency scan experiment is described by virtual modes with $\operatorname{Re} \boldsymbol{k}^{(1)} \,||\, \operatorname{Im} \boldsymbol{k}^{(1)}$.

It should be mentioned that there exist further relations which are often used as boundary conditions for the determination of virtual modes from the dispersion relation. One example is the pure temporal damping with the condition

$$\operatorname{Im} k_{||} = 0 \,. \tag{9}$$

However, it was shown above that this type of virtual modes is not related to any ATR experiment. From this short discussion it is to be seen that the virtual mode treatment depends on the actual experimental conditions. Therefore, the virtual mode treatment only yields special but most important results about the ATR experiment.

In the past this direct relation to the experiment was often absent resulting in some confusion in the connection between calculated virtual modes and measured ATR spectra [34 to 37]. There are a number of studies which impose boundary conditions like pure spatial or temporal damping in an ad hoc way.

5. The Virtual Modes of Type I and Type II

In the following we consider only the case of angle scan. We want to describe ATR experiments on LRSP's with the virtual mode theory. The aim of our work is to include both intrinsic and radiative damping of these modes. Furthermore our treatment shall give a good description of the ATR spectrum and we also want to find out the corresponding optimum conditions for the experiment. To do this we start with two different types of virtual modes.

5.1 Type I: $E^{\mathrm{I}} = 0$

From the ATR response function $1 - R$ we derive the dispersion relation by setting the denominator equal to zero as described at the beginning of Section 4. Then the dispersion relation is given by

$$\begin{aligned}&(\alpha_2\varepsilon_1 - \alpha_1\varepsilon_2)\left((\alpha_2\varepsilon_3 + \alpha_3\varepsilon_2)(\alpha_3\varepsilon_4 + \alpha_4\varepsilon_3) + \right.\\&\quad + \exp(-2\alpha_3 a)(\alpha_2\varepsilon_3 - \alpha_3\varepsilon_2)(\alpha_3\varepsilon_4 - \alpha_4\varepsilon_3)\Big) -\\&\quad - \exp(-2\alpha_2 d)(\alpha_2\varepsilon_1 + \alpha_1\varepsilon_2)\left((\alpha_2\varepsilon_3 - \alpha_3\varepsilon_2)(\alpha_3\varepsilon_4 + \alpha_4\varepsilon_3) + \right.\\&\quad + \exp(-2\alpha_3 a)(\alpha_2\varepsilon_3 + \alpha_3\varepsilon_2)(\alpha_3\varepsilon_4 - \alpha_4\varepsilon_3)\Big) = 0 \qquad (10)\end{aligned}$$

with

$$\alpha_i = \left(k_{\parallel}^2 - \varepsilon_i \frac{\omega^2}{c^2}\right)^{1/2}.$$

The fields of the virtual mode are of the form $\exp(\alpha_1 z)$ in the prism region and $\exp(\alpha_4 z)$ in the substrate. According to the boundary conditions (7) for the angle scan we are interested here, the functions α_1 and α_4 are complex. Therefore the mode exhibits an oscillating behaviour in addition to the exponential one in such a way that the above given condition $\mathrm{Re}\, k^{(1)} \cdot \mathrm{Im}\, k^{(1)} = 0$ concluded from (7) is satisfied. But the exact character of the virtual modes is still ambiguous. It depends on the sign of the real and the imaginary part of α_1 and α_4. In order to describe the propagation properties of SP's in the ATR configuration the dominant field character of the virtual mode must be an outgoing one in the prism region and the field must decay exponentially away from the interface into the substrate. The corresponding conditions are

$$\mathrm{Im}\, \alpha_1 > 0 \qquad (11)$$

and

$$\mathrm{Re}\, \alpha_4 > 0\,. \qquad (12)$$

Those solutions of the dispersion relation (10) which fulfil the conditions (11) and (12) we define as the virtual modes of the type I. This type should describe the propagation properties of a surface polariton taking into account the radiative outgoing of energy into the prism region. Hence the amplitude of it must decrease in the direction of propagation (the $+x$ axis), we conclude the validity of

$$\mathrm{Im}\, k_{\parallel} > 0\,. \qquad (13)$$

Another important point is connected with the sign of the real part of α_2.

The physical procedure valid for surface modes in unperturbed systems in the absence of the prism is to require that the conditions $\mathrm{Re}\, \alpha_2 < 0$, $\mathrm{Re}\, \alpha_4 > 0$ and $\mathrm{Im}\, k_{\parallel} > 0$ must be fulfilled giving an exponential decay of the mode away from the interface into the regions of the outer media and into the direction of propagation. But in the virtual mode treatment modes are considered which describe additionally the radiation loss of the surface polariton (leaky surface wave) due to the presence of the coupling prism (energy radiation into the prism region). In this case the above given requirement for the real part of α_2 must be violated by a requirement for the imaginary part of α_1 (11). In order to describe the experimental situation with the virtual mode theory we are forced to adopt a reasonable solution with the choice of the signs given by (11) and (12). The resulting modes decay in the direction of propagation because of outgoing parts into the prism region. Therefore the type I virtual modes describe correctly the main physical properties of SP propagation in the presence of a prism which takes away energy from the SP by radiation.

5.2 Type II: $E^{\mathrm{II}} = 0$

In contrast to the type I virtual mode we are now looking for a virtual mode which describes the excitation properties of a surface polariton. From the ATR response

function $1 - R$ we derive the dispersion relation for the case that the reflected electric field $\boldsymbol{E}^{\mathrm{r}}$ is equal to zero. This is equivalent to setting the numerator of (1) equal to zero. The resulting dispersion relation for the virtual mode has the form

$$\begin{aligned}&(\alpha_2\varepsilon_1 + \alpha_1\varepsilon_2)\left((\alpha_2\varepsilon_3 + \alpha_3\varepsilon_2)(\alpha_3\varepsilon_4 + \alpha_4\varepsilon_3) + \right.\\&\quad + \exp(-2\alpha_3 a)(\alpha_2\varepsilon_3 - \alpha_3\varepsilon_2)(\alpha_3\varepsilon_4 - \alpha_4\varepsilon_3)\left.\right) -\\&\quad - \exp(-2\alpha_2 d)(\alpha_2\varepsilon_1 - \alpha_1\varepsilon_2)\left((\alpha_2\varepsilon_3 - \alpha_3\varepsilon_2)(\alpha_3\varepsilon_4 + \alpha_4\varepsilon_3) + \right.\\&\quad + \exp(-2\alpha_3 a)(\alpha_2\varepsilon_3 + \alpha_3\varepsilon_2)(\alpha_3\varepsilon_4 - \alpha_4\varepsilon_3)\left.\right) = 0\,. \qquad (14)\end{aligned}$$

In this case the fields are proportional to $\exp(-\alpha_1 z)$ in the prism region and to $\exp(\alpha_4 z)$ in the substrate. Corresponding to the boundary conditions (7) for the angle scan the functions α_1 and α_4 are complex. Since we are interested in the excitation properties of a surface polariton in the ATR configuration the virtual mode must have the character of an incident wave in the prism region and the fields must decay exponentially away from the interface into the substrate. Taking into account the fields given above this behaviour is realized by the conditions

$$\operatorname{Im}\alpha_1 > 0 \qquad (15)$$

and

$$\operatorname{Re}\alpha_4 > 0\,. \qquad (16)$$

The solutions of the dispersion relation (14) which fulfil the conditions (15) and (16) we define as the virtual modes of the type II. In this case of an amplification of energy in the system also $\operatorname{Im} k_{\|} < 0$ is possible in contrary to the conclusion (13) in the case of type I virtual modes. The chosen conditions ensure that the type II virtual modes describe the excitation properties of a surface polariton in the ATR configuration.

6. Discussion

For numerical work we have chosen a SF-59 coupling prism with $\varepsilon_1 = 3.77622$ and a Ag layer [38] with $\varepsilon_3 = -18 + i0.47$ at the He-Ne wave length $\lambda = 632.8$ nm. At first we want to discuss the case of a symmetric embedded Ag layer. The dielectric constants of the superstrate (index-matching liquid layer in an appropriate experimental set-up) ε_2 and of the substrate ε_4 are $\varepsilon_2 = \varepsilon_4 = 2.1211$ (fused silica). Fig. 1 shows the calculated ATR spectra for a sample with a 17 nm thick Ag layer for various thicknesses d of the gap between the coupling prism and the silver layer. In this figure the sharp resonance associated with the excitation of a LRSP is to be seen. The half-width $\Delta\theta_1$ at half-minimum of the reflectivity curve decreases with increasing gap d between the Ag layer and the coupling prism. But the minimum reflectivity of the ATR spectra decreases with increasing gap d and shows a minimum for a definite thickness d^* of the gap ($d^* \approx 1300$ nm for the symmetric case given in Fig. 1). Increasing the gap above this value the minimum reflectivity increases continuously. The discussed behaviour is well demonstrated in the three-dimensional representation of the reflectivity $R(\theta_1, d)$ shown in Fig. 2. According to the conditions of the angle scan ATR the real and the imaginary part of the wave vector component $k_{\|}$ are given by

$$\operatorname{Re} k_{\|} = \frac{\omega}{c}\,\varepsilon_1^{1/2}\sin\theta_1^{\min} \qquad (17)$$

and

$$\operatorname{Im} k_{\|} = \frac{\omega}{c}\,\varepsilon_1^{1/2}\cos\theta_1^{\min}\,\Delta\theta_1\,, \qquad (18)$$

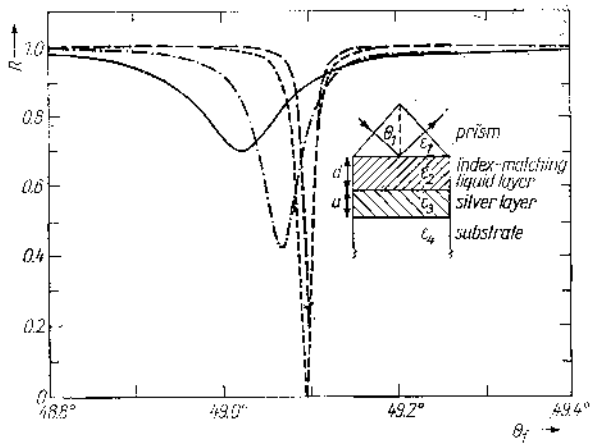

Fig. 1. Calculated ATR spectra of the LRSP existing in the configuration given in the inset of the figure for various thicknesses d of the gap between the silver layer and the coupling prism. $\lambda = 632.8$ nm, $a = 17$ nm. ——— $d = 700$, —·— 900, - - - - 1300, · · · · 1500 nm. $\varepsilon_1 = 3.77622$, $\varepsilon_2 = \varepsilon_4 = 2.12110$, $\varepsilon_3 = -18 + i0.47$

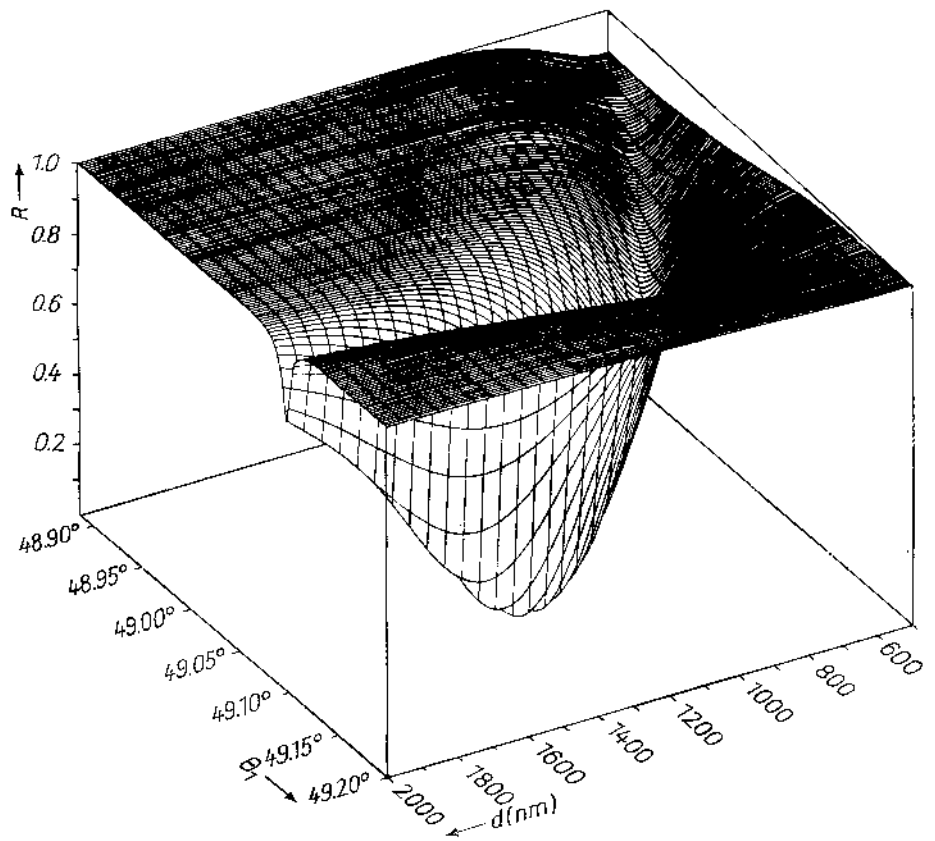

Fig. 2. Three-dimensional representation of the calculated reflectivity $R(\theta_1, d)$ for the configuration given in the inset of Fig. 1

where $\theta_{\mathrm{I}}^{\min}$ is the angle of incidence at the minimum of the reflectivity curve. In Fig. 3 the real and the imaginary parts of $k_{||}$ of virtual modes of type I and II are plotted in dependence of the gap d. It is to be seen that for values of $d < 500$ nm the real part of $k_{||}$ has a minimum and increases sharply for very low values of d. The absolute value of the imaginary part of $k_{||}$ increases up to a maximum and then it decreases with increasing gap d.

As can be seen from Fig. 1, a sensible ATR minimum occurs only for wider gaps d. Therefore in Fig. 4 the results of the real and the imaginary part of $k_{||}$ obtained from the virtual mode treatment (curves) are compared with the results from the ATR spectra (circles) calculated according to (17) and (18) for the gap region $d > 500$ nm. The comparison shows that the results of the ATR calculation are in good agreement with those of the type I virtual mode. That means this virtual mode gives a good description of the propagation properties of the surface polariton. Its propagation length L is defined by

$$L = \frac{1}{2\,|\mathrm{Im}\,k_{||}|}\,. \tag{19}$$

For $d \to \infty$ the system goes over to the unpertubed system (i.e. a semiinfinite superstrate without prism) where no radiative damping occurs. Therefore the propagation length increases up to a value which is determined by the damping of the surface polariton caused by intrinsic processes alone. Comparing Fig. 4a, b, and c it is obvious that the propagation length of the LRSP's decreases with increasing thickness of the Ag layer. In the case of the type II virtual mode the imaginary part of $k_{||}$ becomes zero for a definite value of the gap d which is identical with d^* for which the lowest minimum reflectivity occurs in dependence on the gap d. Furthermore at this point the radiative damping is exactly equal to the intrinsically caused damping of the surface polariton.

In Fig. 5a the complex α_1 plane is shown. The plotted curves represent the values of the real and the imaginary part of α_1 for virtual modes of type I (solid lines) and type II (dashed lines) in dependence on the gap d. It is to be seen that the curve of the type I virtual mode is always determined by $\mathrm{Re}\,\alpha_1 > 0$ and $\mathrm{Im}\,\alpha_1 > 0$. For all values of the gap d the imaginary part of α_1 is much larger than the real part in magnitude. That means in the coupling prism the radiative part of the fields is dominant. Since $\mathrm{Re}\,\alpha_1 > 0$ the type I virtual mode grows exponentially in z-direction in the

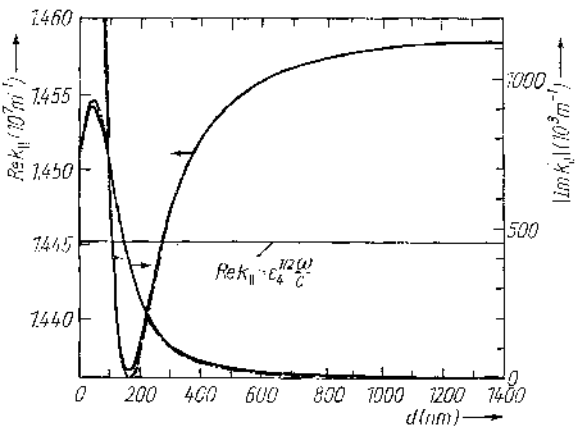

Fig. 3. Real and imaginary part of the wave vector component $k_{||}$ vs. thickness d of the gap between the silver layer and the coupling prism (λ, α, and ε_1 to ε_4 as in Fig. 1). Solid lines represent the results for the virtual mode of type I (———) and dashed lines for the virtual mode of type II (— · · — $\mathrm{Im}\,k_{||} > 0$, $\mathrm{Re}\,k_{||}$; —·— $\mathrm{Im}\,k_{||} < 0$)

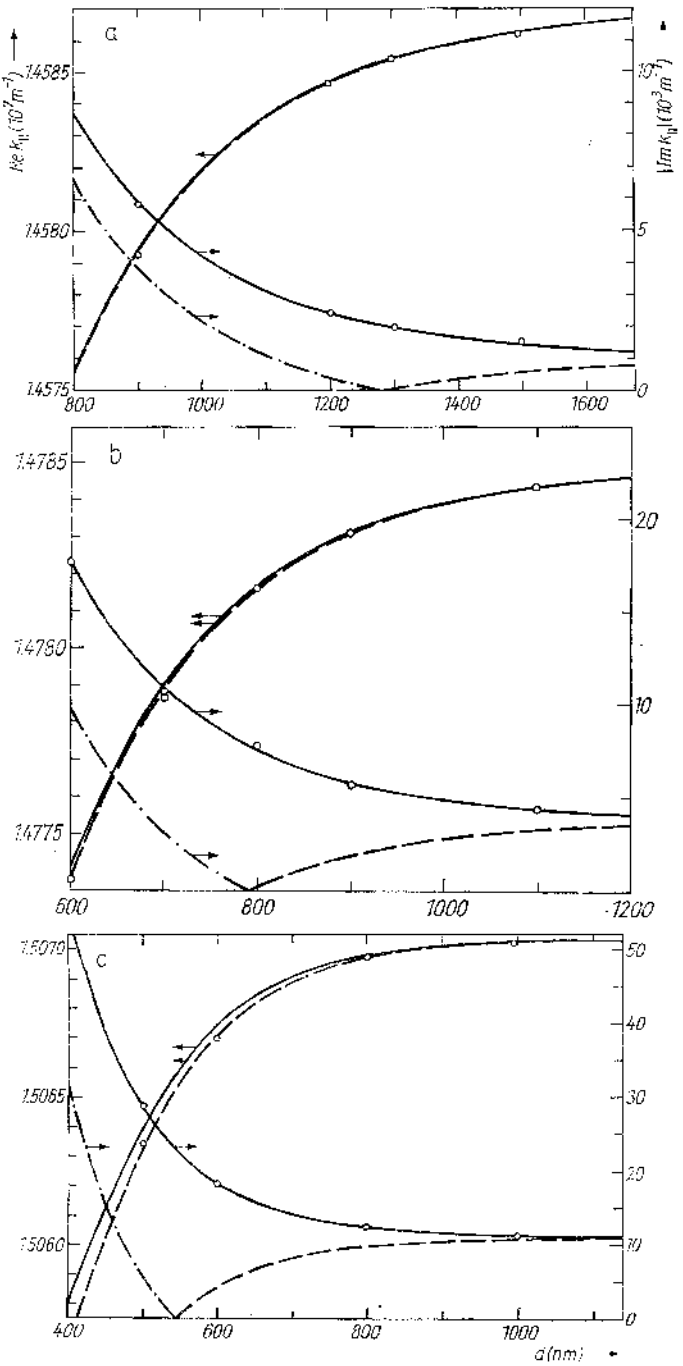

Fig. 4. Real and imaginary part of the wave vector component $k_{\parallel}$ vs. thickness d of the gap between the silver layer and the coupling prism (λ, α, and ε_1 to ε_4 see Fig. 1). Solid lines represent the results for the virtual mode of type I (——), dashed lines for the virtual mode of type II (– – – $\mathrm{Im}\, k_{\parallel} > 0$, $\mathrm{Re}\, k_{\parallel}$; – · – $\mathrm{Im}\, k_{\parallel} < 0$) and the open circles are the results obtained from the calculated ATR spectra. Thickness of the silver layer a) $a = 17$, b) 30, c) 50 nm

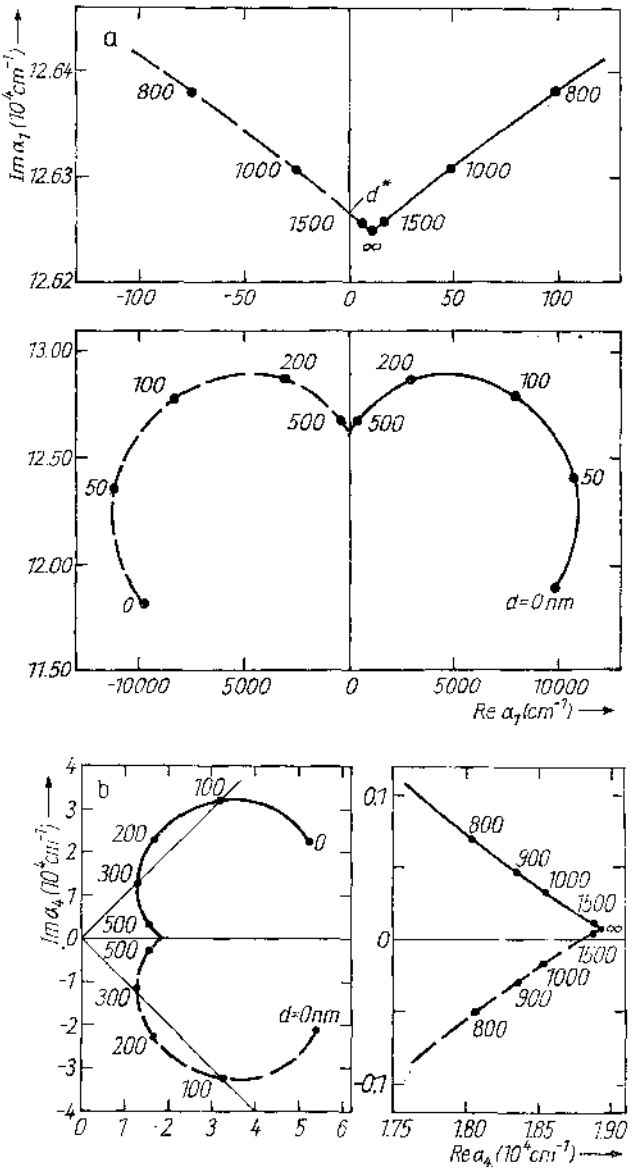

Fig. 5. Loci of a) α_1 and b) α_4 in the complex plane in dependence on the thickness d of the gap between the silver layer and the coupling prism (parameters as in Fig. 1). Type I (———), type II (— · · —)

whole prism region. In the case of the type II virtual mode $\mathrm{Im}\,\alpha_1 > 0$ and $\mathrm{Re}\,\alpha_1 \gtrless 0$ is valid. For the definite value d^* $\mathrm{Re}\,\alpha_1$ vanishes what is related to $\mathrm{Im}\,k_{||} = 0$. For all values of the gap d the imaginary part of α_1 is much larger than the absolute value of the real part of α_1 in magnitude. Following as in the case of type I, the radiative part of the fields in the coupling prism region is dominant. But the type I virtual mode is an outgoing wave and the type II virtual mode is an incoming one for all

thicknesses d of the gap. If the gap d is very large one obtains $\mathrm{Re}\,\alpha_1 > 0$ what is connected with exponentially decaying fields. With decreasing gap d the real part of α_1 becomes negative what results in fields growing exponentially in z-direction. For the definite gap d^* we obtain $\mathrm{Re}\,\alpha_1 = 0$. At this point the fields are neither decaying nor growing, they are ordinary homogeneous plane waves. In Fig. 5 b the corresponding α_4 plane is shown.

From the figure is to be seen that the type I virtual mode is characterized by $\mathrm{Re}\,\alpha_4 > 0$ and $\mathrm{Im}\,\alpha_4 > 0$. For large values of the gap d the real part of α_4 is much larger than the imaginary part in magnitude. Between two fixed values of d (points of intersection of the plotted curve with the line $\mathrm{Re}\,\alpha_4 = \mathrm{Im}\,\alpha_4$) the real part of α_4 is smaller than the imaginary part in magnitude. Consequently the radiative part of the fields in the substrate is dominant and hence the electromagnetic fields are only weakly bound to the interface at $z = 0$.

In the case of the type II virtual mode $\mathrm{Re}\,\alpha_4 > 0$ and $\mathrm{Im}\,\alpha_4 \gtrless 0$ is valid. For the definite value of the gap d^* $\mathrm{Im}\,\alpha_4$ vanishes what is related to $\mathrm{Im}\,k_{\|} = 0$. If the gap d is very large one obtains $\mathrm{Im}\,\alpha_4 > 0$ and the real part of α_4 is very much larger than the imaginary part in magnitude. With decreasing gap d the imaginary part of α_4 becomes negative. Analogous as for the type I between the two fixed values of d (points of intersection of the dashed curve with the line $\mathrm{Re}\,\alpha_4 = -\mathrm{Im}\,\alpha_4$) the real part of α_4 is smaller than the absolute value of the imaginary part. That means the radiative part of the electromagnetic fields in the substrate is dominant and hence the fields are only weakly bound to the interface at $z = 0$. However, in difference to the type I virtual mode the sign of the imaginary part of α_4 is negative what is connected with an outgoing wave. Therefore the character of the type II virtual mode changes from an incoming to an outgoing wave whereas the type I virtual mode is an incoming wave for all thicknesses of the gap d. In Fig. 5 that part of the complex α-planes which is related to the ATR experiment, we have additionally shown in an enlarged fashion. From the discussion given above it is clear that the virtual modes exhibit in general an oscillating behaviour in the regions 1 and 4.

In Fig. 6 the various fields of the virtual modes are illustrated. The type I virtual mode is in the prism region an outgoing wave with exponentially growing fields. In the substrate the wave is an incoming one and the fields decay exponentially from the interface. Since the media 1 and 4 are lossless (i.e. ε_1 and ε_4 are real quantities) the planes of constant phase of these inhomogeneous waves are perpendicular to the planes of constant amplitude. The dominant character is the radiative in the prism region and the exponentially decaying in the substrate. That means the character of the type I virtual mode is that of a surface wave which radiates energy into the prism region. The amplitude of this virtual mode decreases in the direction of propagation. For the type II virtual mode the field structure is shown for three typical thicknesses of the gap d. In the prism region the character of the field changes from an exponentially decaying for large values of d to an exponentially growing one for small values of d. The fields have the character of incoming waves in all cases. In the substrate the fields are always exponentially decaying but the character is changed from an incoming wave of large values of d to an outgoing wave for small values of d. In the special case of $\mathrm{Re}\,\alpha_1 = \mathrm{Im}\,\alpha_4 = 0$ the type II virtual mode has the field of an incoming plane wave in the prism region and it decays pure exponentially in the substrate. That means the dominant character of the fields of type II virtual modes is that of a surface polariton excited by a driving field in region 1. Consequentely the two types of virtual modes which was introduced here describe the physics of the excitation and the propagation of a surface polariton very well.

Now we want to discuss the asymmetric case that means we consider $\varepsilon_2 < \varepsilon_4$ with

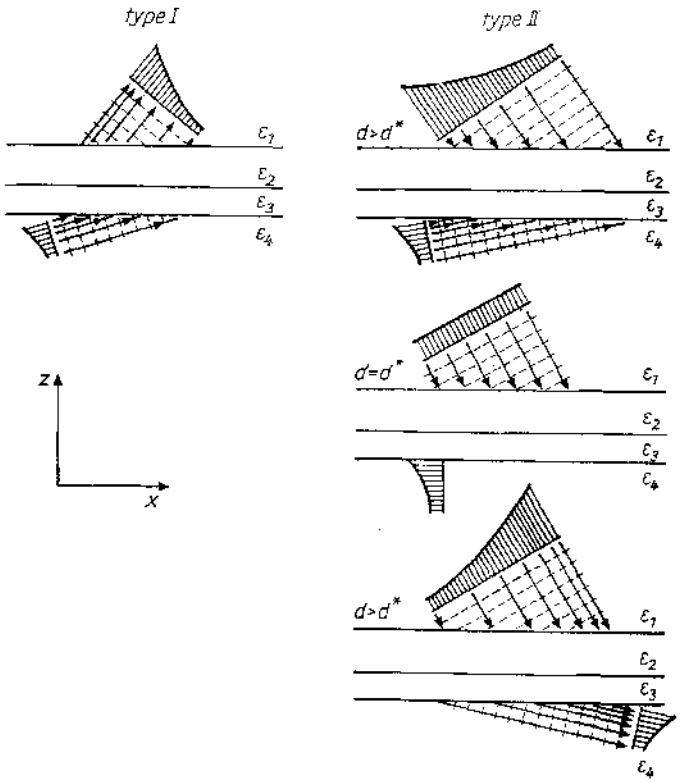

Fig. 6. Varieties of the fields of the virtual mode. Solid and dashed lines correspond to equiamplitude and equiphase contours, respectively. The field amplitude variation is suggested by the striped exponential profiles

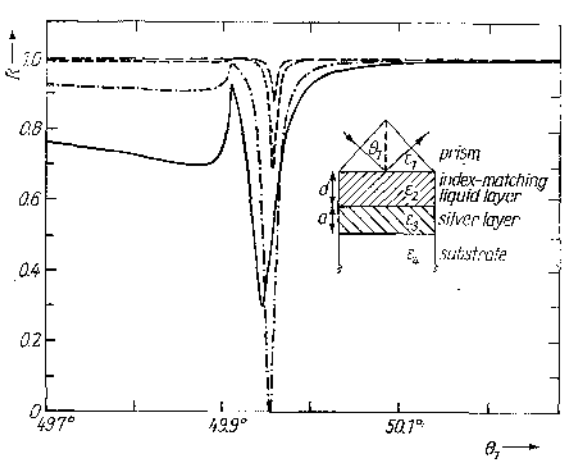

Fig. 7. Calculated ATR spectra of the LRSP existing in the configuration given in the inset of the figure for various thicknesses $\bar{d}$ of the gap between the silver layer and the coupling prism. λ = = 632.8 mm, a = 17 nm. ——— $\bar{d}$ = 700, — · — 900, - - - - 1300, — — — 1500 nm. ε_1 = 3.77622, ε_2 = 2.12110, ε_3 = −18 + i0.47, ε_4 = 2.2100

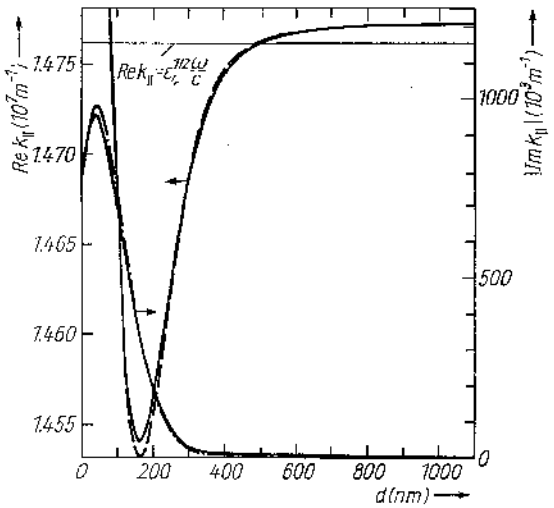

Fig. 8. Real and imaginary part of the wave vector component $k_{||}$ vs. thickness d of the gap between the silver layer and the coupling prism (parameters as in Fig. 7). Solid lines represent the results for the virtual mode of type I (· · · ·) and dashed lines for the virtual mode of type II (— — — Im $k_{||} > 0$, Re $k_{||}$; —·— Im $k_{||} < 0$)

respect to the ATR experiment. In Fig. 7 calculated ATR spectra are plotted for a sample with a 17 nm thick silver layer for various thicknesses d of the gap. The sharp resonance in the reflectivity is associated with the excitation of a LRSP in this configuration.

For a critical angle of incidence (when $(\mathrm{Re}\, k_{||})^2 < \varepsilon_4 \omega^2/c^2$) the wave becomes quite radiative in the substrate. The consequence is a drastic decreasing of the reflectivity what is to be seen on the left side of the curves in Fig. 7. The behaviour of the ATR minimum in dependence of the thickness d of the gap is in principle the same as in the symmetric case. For a definite value of the gap d^* the minimum reflectivity is almost equal to zero ($d^* \approx 900$ nm cp. Fig. 7) and it increases when the thickness of the gap exceeds or falls below this value. Comparing the ATR spectra for the symmetric (Fig. 1) and the asymmetric case (Fig. 7) it is to be seen that the half-width of the reflectivity

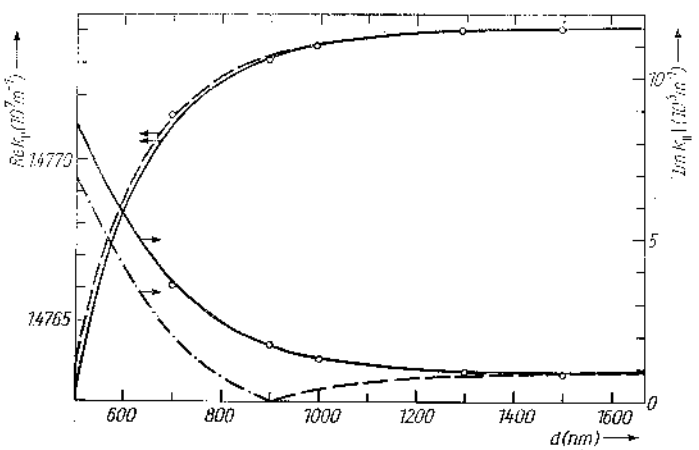

Fig. 9. Real and imaginary part of the wave vector component $k_{||}$ vs. thickness d of the gap between the silver layer and the coupling prism. Solid lines represent the results for the virtual mode of type I (———), dashed lines for the virtual mode of type II (— — — Im $k_{||} > 0$, Re $k_{||}$; —·— Im $k_{||} < 0$) and the open circles are the results obtained from the calculated ATR spectra

minimum is smaller in the asymmetric case. In Fig. 8 the real and imaginary part of the wave vector component $k_{||}$ of type I and type II virtual modes are shown in dependence on the gap d. For thicknesses of the gap $d > 500$ nm the real part varies only weakly with d. Therefore in the asymmetric case the so-called dielectric shift which describes the difference of the real part of $k_{||}$ calculated from the ATR spectra to that calculated for the unperturbed system (without prism for $d \to \infty$), is only small.

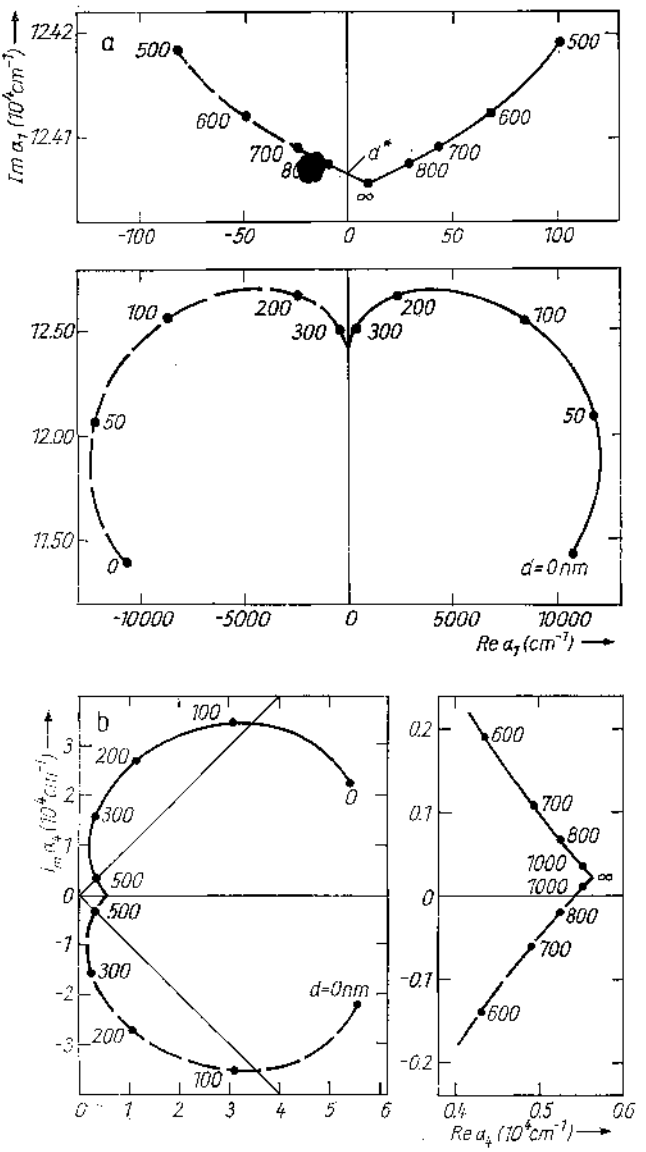

Fig. 10. Loci of a) α_1 and b) α_4 in the complex plane in dependence on the thickness d of the gap between the silver layer and the coupling prism (parameters as in Fig. 7). Type I (———), type II (– – – –)

For values of d for which $(\mathrm{Re}\, k_{||})^2 < \varepsilon_4 \omega^2/c^2$ is valid, the behaviour of the plotted curves is qualitatively the same as in the symmetric case. More detailed information about the real and the imaginary part of $k_{||}$ in the interesting region of the gap d is shown in Fig. 9. The main result is that due to the asymmetry lower values of the imaginary part of $k_{||}$ and therefore higher values of the propagation length of the LRSP's can be reached. In Fig. 10 the loci of α_1 and α_4 in the complex plane are plotted in dependence on the gap d for the asymmetric configuration. They show in principle the same behaviour as discussed in connection with Fig. 5.

To investigate systematically the effect of an asymmetric embedding of the thin Ag layer in the presence of the coupling prism we need a criterion on the free parameter d. In order to compare the obtained results for various differences $\Delta\varepsilon$ between ε_2 and ε_4, we chose the thickness of the gap d^* for which the imaginary part of $k_{||}$ of the type II virtual mode vanishes. At this thickness of the gap the radiative and the intrinsically caused damping are equal to each other. That means the damping in such a configuration is double the value as the damping in the unpertubed configuration because there is no radiative part. Consequently the propagation length in the configuration with prism and the gap d^* is reduced to one half of the propagation length in the unpertubed configuration. All calculation we have made for the unperturbed configuration [25] can therefore be transferred to the configuration with prism and the gap d^*. That means, also in the configuration with prism a high increase in the propagation length of the LRSP can be reached due to asymmetric embedding of an Ag layer. This behaviour is illustrated in Fig. 11.

From the figure is further to be seen that for the ATR configuration the stop-points of the curves $L(\varepsilon_4)$ are shifted towards lower values of ε_4 for fixed ε_2. The reason for this behaviour is that with increasing $\Delta\varepsilon$ the thickness of the gap d^* shifts toward that thickness for which $(\mathrm{Re}\, k_{||})^2 = \varepsilon_4 \omega^2/c^2$ of the virtual mode is valid (see Fig. 9). The last thickness is the limiting one for the performance of an ATR experiment because in the case of $(\mathrm{Re}\, k_{||})^2 < \varepsilon_4 \omega^2/c^2$ the field in the substrate is quite a radiative one. In an experimental set-up it is possible to use larger thicknesses of the gap d. Then the radiative damping will be smaller but contrary to this the minimum reflectivity of the ATR resonance increases.

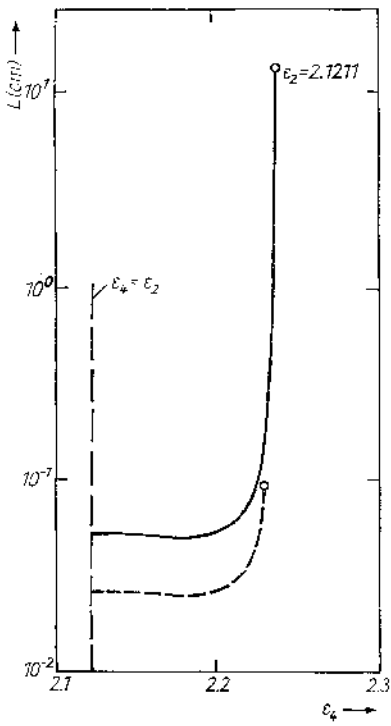

Fig. 11. Propagation length L of LRSP's existing in the configuration given in the inset of Fig. 1 and Fig. 7, respectively, vs. dielectric constant ε_4 of the substrate. The solid line represents the results for the configuration without prism [25] and the dashed line for the configuration with the coupling prism separated by the gap d from the silver layer

7. Conclusion

In our paper we have given a detailed analysis of damping properties of surface polaritons, especially long-range surface plasmon-polaritons (LRSP). Effects of surface roughnesses and finite beam width are not taken into account. The aim of our work was to show the possibilities of the virtual mode theory to model ATR experiments. Using these possibilities we have investigated the damping properties of LRSP's in asymmetric layer structures in the presence of a coupling prism. The following results are obtained:

(i) The virtual mode of the type I gives a very good description of the propagation properties of LRSP's in the presence of a coupling prism. This virtual mode includes both intrinsic and radiative damping.

(ii) The virtual mode of the type II gives a very good description of the excitation process of SP's. This type describes a SP with a driving field. With the type II virtual mode optimum condition for an ATR experiment can be found out.

(iii) In the presence of the coupling prism and following with regard to radiative damping the propagation length in the asymmetric configuration exceeds the value for the symmetric case significantly.

References

[1] A. Otto, Z. Phys. **216**, 398 (1968).
[2] D. J. Evans, S. Ushioda, and J. D. McMullen, Phys. Rev. Letters **31**, 1369 (1973).
[3] K. L. Kliewer and R. Fuchs, Adv. chem. Phys. **27**, 355 (1974).
[4] R. Ruppin and R. Englman, Rep. Progr. Phys. **33**, 149 (1970).
[5] D. N. Mirlin, in: Surface Polaritons, Ed. V. M. Agranovich and D. L. Mills, North-Holland Publ. Co., Amsterdam 1982 (p. 3).
[6] G. Borstel and H. J. Falge, phys. stat. sol. (b) **88**, 11 (1977).
[7] G. Borstel and H. J. Falge, in: Electromagnetic Surface Modes, Ed. A. D. Boardman, John Wiley & Sons, 1982 (p. 219).
[8] G. N. Zhizhin, M. A. Moskalova, E. V. Shomina, and V. A. Yakovlev, see [5] p. 93.
[9] J. Schoenwald, E. Burstein, and J. M. Elson, Solid State Commun. 12, 185 (1973).
[10] R. J. Bell, R. W. Alexander, W. F. Parks, and G. S. Kovener, Optics Commun. 8, 147 (1973).
[11] Z. Schlesinger and A. J. Sievers, Solid State Commun. **43**, 671 (1982).
[12] M. Fukui, C. V. Y. So, and R. Normandin, phys. stat. sol. (b) 91, K61 (1979).
[13] D. Sarid, Phys. Rev. Letters **47**, 1927 (1981).
[14] Z. Lenac and M. S. Tomaš, J. Phys. C **16**, 4273 (1983).
[15] L. Wendler and R. Haupt, J. Phys. C **19**, 1871 (1986).
[16] D. Sarid, IEEE J. Quantum Electronics **20**, 943 (1984).
[17] G. I. Stegeman, J. J. Burke, and D. G. Hall, Appl. Phys. Letters **41**, 906 (1982).
[18] R. T. Deck and D. Sarid, J. Opt. Soc. Amer. **72**, 1613 (1982).
[19] H. Dohi, Y. Kuwamura, M. Fukui, and O. Tada, J. Phys. Soc. Japan **53**, 2828 (1984).
[20] J. C. Quail, J. R. Rako, and H. J. Simon, Optics Letters 8, 377 (1983).
[21] Y. Kuwamura, M. Fukui, and O. Tada, J. Phys. Soc. Japan **52**, 2350 (1983).
[22] A. E. Craig, G. A. Olson, and D. Sarid, Optics Letters **8**, 380 (1983).
[23] J. C. Quail, J. G. Rako, H. J. Simon, and R. T. Deck, Phys. Rev. Letters **50**, 1987 (1983).
[24] J. C. Quail and H. J. Simon, J. appl. Phys. **56**, 2592 (1984).
[25] L. Wendler and R. Haupt, J. appl. Phys. **59**, 3289 (1986).
[26] A. Otto, Adv. Solid State Phys. **14**, 1 (1974).
[27] A. Otto, in: Optical Properties of Solids, New Developments, Ed. B. O. Seraphin, North-Holland Publ. Co., Amsterdam 1975 (p. 677).
[28] E. Kretschmann, Z. Phys. **241**, 313 (1971).
[29] G. S. Kovener, R. W. Alexander, Jr., and R. J. Bell, Phys. Rev. B **14**, 1458 (1976).

[30] K. L. KLIEWER and R. FUCHS, Phys. Rev. **150**, 573 (1966).
[31] P. E. FERGUSON, R. F. WALLIS, M. BELAKHOVSKY, J. P. JADOT, and J. TOMKINSON, Surface Sci. **76**, 483 (1978).
[32] P. E. FERGUSON, R. F. WALLIS, and G. CHAUVET, Surface Sci. **82**, 255 (1979).
[33] G. N. ZHIZHIN, S. A. KISELEV, and M. A. MOSKALOVA, Optika i Spectroskopiya **58**, 916 (1985).
[34] P. F. ROBUSTO and R. BRAUNSTEIN, phys. stat. sol. (b) **107**, 127 (1981).
[35] P. F. ROBUSTO and R. BRAUNSTEIN, phys. stat. sol. (b) **107**, 443 (1981).
[36] Y. YOKOTA, M. FUKUI, and O. TADA, J. Phys. Soc. Japan **53**, 2833 (1984).
[37] R. C. BELL, R. W. ALEXANDER, JR., C. A. WARD, and I. L. TYLER, Surface Sci. **48**, 253 (1975).
[38] P. B. JOHNSON and R. W. CHRISTY, Phys. Rev. B **12**, 4370 (1972).

(Received December 16, 1986)